Title

Spin-resolved photoemission study of epitaxially grown MoSe2 and WSe2 thin films

Journal

Journal of Physics Condensed Matter, 28(45)

ISSN

0953-8984

Authors

Mo, Sung-Kwan

Hwang, Choongyu

Zhang, Yi

et al.

Publication Date

2016-11-16

DOI

10.1088/0953-8984/28/45/454001

Peer reviewed

Spin-resolved photoemission study of epitaxially grown $MoSe_2$ and WSe_2 thin films

Sung-Kwan Mo[1], Choongyu Hwang[2], Yi Zhang[1,3,4], Mauro Fanciulli[5,6], Stefan Muff[5,6], J. Hugo Dil[5,6], Zhi-Xun Shen[4,7] and Zahid Hussain[1]

[1] Advanced Light Source, Lawrence Berkeley National Laboratory, Berkeley, CA 94720, USA
[2] Department of Physics, Pusan National University, Busan 609-735, Korea
[3] National Laboratory of Solid State Microstructures, School of Physics, Collaborative Innovation Center of Advanced Microstructures, Nanjing university, Nanjing 210093, China
[4] Stanford Institute of Materials and Energy Sciences, SLAC National Accelerator Laboratory, Menlo Park, CA 94025, USA
[5] Institut de Physique, Ecole Polytechnique Fédérale de Lausanne, CH-1015 Lausanne, Switzerland
[6] Swiss Light Source, Paul Scherrer Institut, CH-5232 Villigen, Switzerland
[7] Geballe Laboratory for Advanced Materials, Departments of Physics and Applied Physics, Stanford University, Stanford, CA 94305, USA

E-mail: SKMo@lbl.gov

Abstract. $MoSe_2$ and WSe_2 with a few layer thickness possess non-trivial spin texture with sizable spin splitting due to the inversion symmetry breaking embedded in the crystal structure and strong spin-orbit coupling. We report spin-resolved photoemission study of the $MoSe_2$ and WSe_2 thin film samples epitaxially grown on bilayer graphene substrate. We found spin polarization only in single- and tri-layer samples, but not in bi-layer sample, mostly along the out-of-plane direction of the sample surface. The measured spin polarization is found to be strongly dependent on the light polarization as well as the measurement geometry, which reveals intricate coupling between spin and orbital degrees of freedom in this material class.

PACS numbers: 73.22.-f, 79.60.-i, 73.20.-r

Keywords: transition metal dichalcogenides, $MoSe_2$, WSe_2, ARPES, photoemission, spin resolved photoemission

Journal Reference - J. Phys.: Condens. Matter 28, 454001 (2016).

1. Introduction

Two-dimensional (2D) materials, such as graphene, hBN, phosphorene, and transition metal dichalcogenides (TMDCs), are the platform for new physical properties that are not attainable in their bulk counterparts [1, 2, 3, 4]. They often exhibit versatile electronic structure controllable by thickness, surface chemical adsorption, and strain [5, 6, 7]. They can also be stacked into heterostructures to develop a new state in the interfaces [8] as well as through proximity effect [9]. Of particular interest is the TMDC, MX_2 (M= Mo, W; X= S, Se) semiconductor with unique properties in a few layer limit, such as indirect to direct band gap transition [10, 11], large exciton binding energy [12, 13, 14], well-defined valley degrees of freedom [15, 16, 17, 18], and spin-splitting of the valence band (VB) [19, 20, 21]. Many effort has been made to harvest these properties into practical optoelectric, spintronic, and valleytronic devices [22, 23, 24].

The hallmark of the electronic structure of MX_2 is the spin-splitting of the VB at the K/K'-point of the hexagonal Brillouin zone and concomitant spin-valley locking [14, 15, 16, 20]. A single layer of MX_2 is made of a layer of M atoms in a trigonal prismatic coordination sandwiched by two layers of X atoms. When the thickness is reduced to the single layer (1ML), the inversion symmetry is naturally broken. Combined with strong spin-orbit coupling (SOC), this leads to a sizable Rashba-type spin-splitting as well as a strong spin-valley coupling with distinct real spin indices at the K/K'-point [17]. Inversion symmetry is recovered in bi-layers (2ML) making the VB spin-degenerate. With tri-layer (3ML) of thickness, the inversion symmetry is broken again but with less pronounced spin polarization compared to that in 1ML [20].

Angle-resolved photoemission (ARPES) is one of the most suitable tool to investigate the electronic structure of 2D materials with energy and momentum resolution as well as surface sensitivity [25]. There have been a number of ARPES studies either on bulk MX_2 samples [26, 27, 28] or a few layer samples [20, 21, 29, 30] prepared by various methods such as exfoliation, chemical vapor deposition (CVD), and epitaxial growth. They all observe sizable splitting in VB at the K-point, with size $\sim$ 170 meV for MoS_2 and $MoSe_2$ and $\sim$ 450 meV for WS_2 and WSe_2 as W induces larger SOC. However, due to the spin-integrated nature of their spectra, one cannot really conclude that these are spin-split bands purely from the experimental data unless supported by theoretical calculations, and cannot directly deduce the nature of spin texture of each band.

The additional information on spin polarization can be obtained through spin-resolved ARPES (SARPES) [31, 32, 33] as has been shown for topological surface states in topological insulators [34, 35, 36]. There has been only a few SARPES studies on MX_2 [37, 38, 39] despite the large interest on the material class, mainly due to the difficulty in preparing large area samples suitable for measurements in ultra-high vacuum environment, as current SARPES setups at the synchrotron source are bound to large beam spot size to allow maximum photon flux. Moreover, the previous SARPES works are still essentially on bulk samples of MX_2, such as bulk inversion symmetry broken 3R phase of MoS_2 [37] or spin polarization induced by the space charge residing in the overlayer [38]. Of particular interest, Ref. [39] reports spin polarized signal just from regular bulk WSe_2, and interprets their results in terms of strong electron localization at the K/K'-point of WSe_2.

In this paper, we present SARPES data measured on a few layer $MoSe_2$ and WSe_2 samples, grown by molecular beam epitaxy (MBE) on bilayer graphene (BLG) substrate with exact layer-by-layer thickness control. We found the spin polarization lies mostly in the out-of-plane direction of the sample surface in 1ML samples of both $MoSe_2$ and WSe_2, albeit the degree of polarization is not as much as proposed by theory. The spin polarization disappears and reappears as thickness increases to 2ML and 3ML following the recovery and breaking of inversion symmetry. We found the valley dependent spin flip between K and K' points only in particular geometry, which indicate the existence of non-trivial geometric effect in our SARPES signal. We also found light polarization dependent flip of spin polarization due to the intricate coupling between spin and orbital degrees of freedom.

2. Experimental

Thin film samples of $MoSe_2$ with 1ML, 2ML and 3ML thicknesses and WSe_2 with 1ML thickness were grown using molecular beam epitaxy (MBE) on bilayer graphene substrate at the Beamline 10.0.1, Advanced Light Source, Lawrence Berkeley National Laboratory.

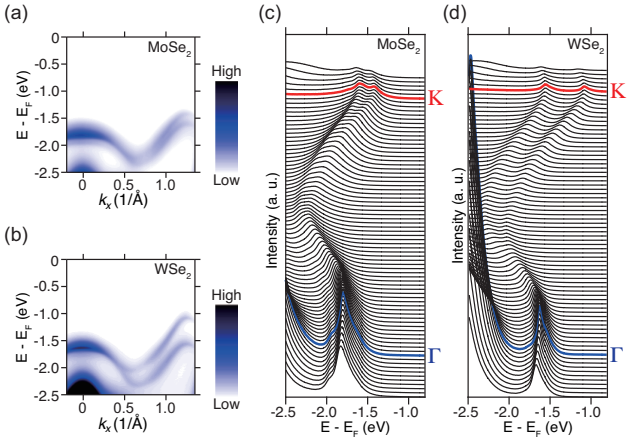

Figure 1. (Color Online) Spin-integrated ARPES spectra of 1ML $MoSe_2$ and WSe_2 measured with 70eV photons at 60K. (a), (b) Intensity map along the Γ-K direction of the hexagonal Brillouin zone. (c), (d) EDC stacks along the same direction. Both shows monolayer feature at the Γ-point and clear splitting at the K-point.

The number of layers, crystallographic phase, and surface quality were monitored using Reflection High-Energy Electron Diffraction (RHEED), Low-Energy Electron Diffraction (LEED), and *in situ* spin-integrated ARPES. The details of the growth condition and the sample characterization were the same as described in Ref. [20] and [21]. The samples were then capped with amorphous Se with thickness $\sim$ 100 Å for the transfer to SARPES system.

SARPES measurements were performed at the COPHEE endstation of the SIS beamline at the Swiss Light Source, equipped with an Omicron EA125 analyzer and a pair of orthogonally mounted 40kV Mott detectors [40]. The sample temperature and the base pressure were 20K and 3 $\times$ 10^{-10} mbar, respectively. The Se capping layer was removed by heating the sample to 300°C for 30 minutes right before the measurement. The absence of residual Se was confirmed by measuring the ARPES intensity at the Fermi energy. The sample alignment and the K-point position were calibrated with LEED and spin-integrated ARPES scans. Photon energies ranging from 30eV to 55eV were used for the measurements, and no significant photon energy dependence were found within the limited set of photon energies used. However, this does not eliminate the possibility of photon energy dependent final state effect in the SARPES process in this material. Only the SARPES spectra measured with 55eV are shown in this paper.

3. Data and Discussion

3.1. Spin integrated spectra of 1ML $MoSe_2$ and WSe_2

Fig. 1 shows the overall electronic structure of 1ML $MoSe_2$ and WSe_2 from spin-integrated ARPES spectra along the Γ-K direction of the surface hexagonal Brillouin zone. The key features of the monolayer MX_2 electronic structures are clearly visible both in energy-momentum intensity maps in Fig. 1 (a), (b) and stacks of energy distribution curves (EDCs) in Fig. 1 (c), (d). First, there exists only a single branch of bands at the Γ-point. The number of branches of the Γ-point band increases following the number of layers [20, 21]. Second, there exists a clear splitting in the valence band at the K-point. The size of these splitting is much larger in WSe_2 $\sim$ 470 meV compared to that in $MoSe_2$ $\sim$ 180 meV, due to the stronger SOC induced by heavier element W. Third, the band maximum at the Γ-point locates at the higher binding energy than that at the K-point, leaving the valence band maximum at the K-point. Combining this with the conduction band minimum being at the K-point in the unoccupied state [20, 21, 26], the 1ML $MoSe_2$ and WSe_2 are direct band gap semiconductors.

In the following discussions regarding SARPES data, we will focus mostly on the split valence band feature at the K-point, which is proposed to be spin polarized [17, 19, 20].

3.2. Spin resolved spectra of 1ML $MoSe_2$ and WSe_2

In Fig. 2, we present the SARPES data at the K-point of 1ML $MoSe_2$ and WSe_2. We first show the schematic drawing of the experimental geometry along with the definition of xyz coordinates in the sample reference frame in Fig. 2(a). The angle between the incident photon momentum and the outgoing electrons is fixed at 45°. Different k-points in momentum space can be reached by rotating the samples in all three axes, tilt (around x axis), polar (around y axis), and azimuth (around z axis). The spectra are measured with 55 eV photons with C+ photon polarization unless otherwise noticed.

The spin resolved EDCs along with the polarization, which is the difference between the up-spin intensity and the down-spin intensity divided by the sum of two, are presented for x, y, and z directions for 1ML $MoSe_2$ (Fig. 2 (b) - (d)) and for 1ML WSe_2 (Fig. 2 (e) - (g)). One immediately notices that the major component of the spin polarization is along the z direction, the out-of-plane direction from the sample surface, while there exist slight in-plane components that cannot be explained by simple experimental uncertainty. This is particularly clear in WSe_2 case, in which the splitting between two valence band peaks

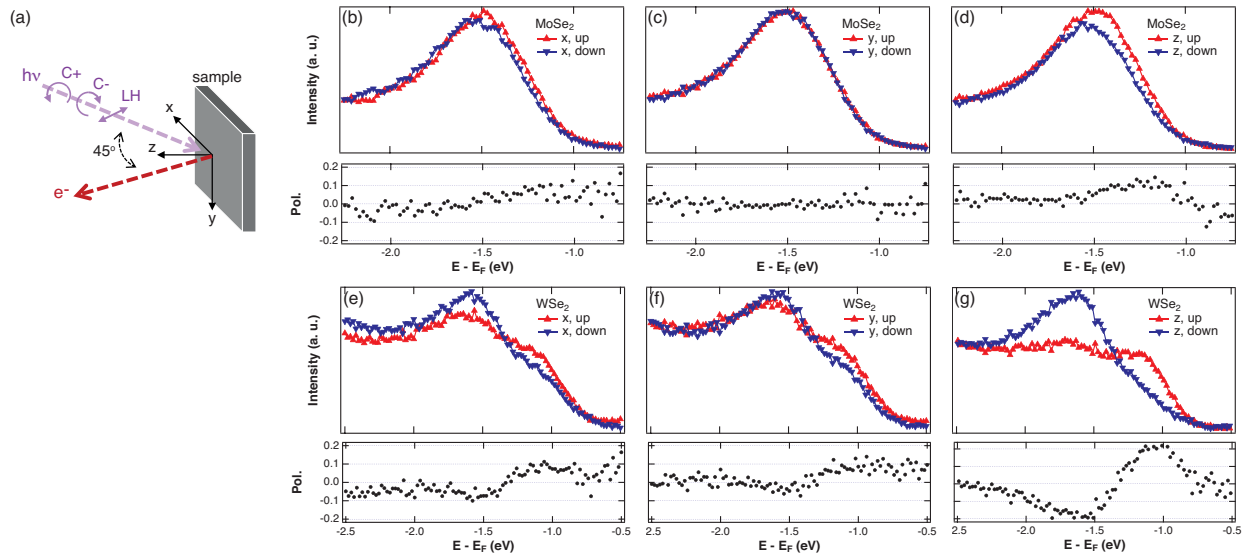

Figure 2. (Color Online) (a) Schematic diagram to show the measurement geometry. (b) - (d) SARPES EDC intensity and polarization of 1ML $MoSe_2$ along x, y, and z directions at the K-point. (e) - (g) SARPES EDC intensity and polarization of 1ML WSe_2 along x, y, and z directions at the K-point.

is large enough to overcome inevitable limited resolution of SARPES data. The intrinsic inefficiency of SARPES process forced us to use less collimated synchrotron light to allow maximum amount of photons to reach the sample, which is translated into poorer resolution from the beamline compared to spin-integrated ARPES as well as a large spot size at the sample. For $MoSe_2$ the spin polarization is not as clear as that in WSe_2 as 180 meV splitting is now comparable to the energy resolution of the measurement, but still the polarization along z direction particularly of the lower binding energy peak $\sim$ -1.4 eV is identifiable. The major component of spin polarization being along the z direction is consistent with previously reported SARPES work on bulk WSe_2[39].

In theory [17, 19, 20], we expect to see the spin polarization only along the z direction at the K-point valence band maximum. The observed small amount of in-plane component indicate the existence of spin state interference [41] between the different spin states of the K-point split bands, which can give non-zero spin component along x and y direction for the measured spin texture in SARPES. Similar effect has been commonly observed in SARPES measurement, such as in the surface state of Rashba alloy Sb/Ag(111) [41] and the topological surface state of Bi_2Se_3 [42].

Another interesting aspect of our SARPES data is that the maximum amount polarization is only $\sim$ 20%, even in WSe_2 where clear separation between spin polarized peaks exists, as opposed to nearly 100 % expected from theoretical calculations [20]. We attribute this mainly to the limited resolution and the intrinsic broadening inherent in SARPES, which gives overlap of the two spin polarized states to reduce the measured spin polarization. Another contributing factor is the spin independent or unpolarized background, due to the secondary scattering of the photoelectrons, which also decreases the measured spin polarization.

We also need to consider the existence of mirror twin domains, universal in MX_2 samples. The single layer MX_2 has 3-fold rotational symmetry since M and X atoms occupy alternating hexagonal corners at different height. The growth process therefore naturally favors triangular domains as is clearly shown in CVD grown samples and nanoparticles of MX_2 [43, 44]. Our MBE grown samples are bound to have a mixture of the domains with triangle point up (up-triangle domain) and its mirror twin domain pointing downwards (down-triangle domain), since they are energetically degenerate. Although such mirror twin domain gives interesting properties at the boundary [45, 46], it also acts to reduce the measured polarization in SARPES since the signal from K-point always mixes with that from K'-point.

3.3. Thickness dependence of spin ARPES in $MoSe_2$

Now we move on to the thickness dependence of the SARPES spectra in $MoSe_2$ thin film samples. Since we have established that the major spin polarization component is along the z direction, we will only compare z component of SARPES data and spin polarization in subsequent subsections.

Spin resolved EDCs and spin polarization at the K-point along z direction are shown in Fig. 3 for 2ML

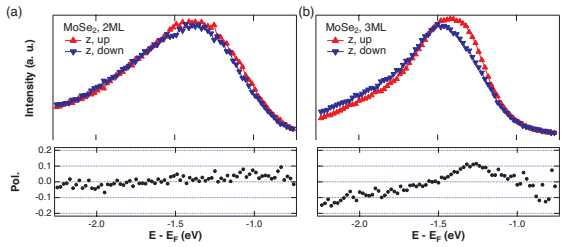

Figure 3. (Color Online) SARPES spectra of 2ML and 3ML $MoSe_2$ at the K-point.

and 3ML $MoSe_2$. As the thickness increases from 1ML shown in Fig. 2(d) to 2, 3MLs, we found the spin polarization along z direction disappears for 2ML but reappears in 3ML along the same direction. It has been theoretically proposed [20] that such oscillatory behavior would occur as the inversion symmetry is restored in 2ML and gets broken again for 3ML. However, the degree of polarization should decrease quite a bit in 3ML compared to 1ML. This is not clearly observable in our data in Fig. 3(b) compared to Fig. 2(d), which is again due to the limited resolution and intrinsic broadening against the small splitting energy.

3.4. Crystal orientation dependence of the spin polarization

In this subsection, we discuss the key aspect of the spin-valley coupling in MX_2, the change in the spin polarization directions in the spin split valence band at different valleys, i.e., the spin flip between K- and K'-point.

Fig. 4 shows the momentum dependence of the spin resolved EDCs and spin polarization along z direction in 1ML WSe_2. Fig. 4(a) is an exact reproduction of the data already shown in Fig. 2(g), which shows up spin polarization for the low energy peak $\sim$ -1.1 eV and down spin polarization for the high energy peak $\sim$ -1.57 eV. Fig. 4(b) is the SARPES data along z direction at the M-point, which clearly shows no spin polarization. The inset in Fig. 4(b) is the schematic drawing to show the definition of K, M, K'(1) and K'(2) points. From the center of the Brillouin zone, the Γ-point, the K- and K'(1)-points can be accessed by changing tilt angles. From the K-point, it requires the rotation of azimuthal angles to reach M- and K'(2)-points.

The K'(1)-point shown in Fig. 4(c) shows clear reversal of spin polarization. The low energy peak $\sim$ -1.1 eV now has down spin polarization while the high energy peak $\sim$ -1.57 eV exhibit up spin polarization. Such a spin flip is as expected from the strong spin-valley locking of MX_2 [15, 16, 17] and is considered as the crucial aspect of the valleytronic application. On the other hand, the spin polarization at the K'(2)-point, reached by the azimuthal rotation from the K-point, shown in Fig. 4(d), does not show such spin flipping.

This apparent discrepancy between supposedly equivalent two momentum points clearly indicates that there exists a non-trivial geometric effect in our SARPES data. The change in flip angle involves the reversal of certain orbital parities with respect to the mirror plane defined by incoming light and outgoing electron momentum, followed by the changes in the sign of SARPES matrix element [47]. The reversal of the measured spin polarization by changing the flip angle suggests that the spin texture prominent in our measurement condition, 55eV, C+ polarized, is sensitive to the orbitals that changes their parity when reflected with respect to the mirror plane. According to the first principle calculations [19, 39], the orbital character of the K-point VB is mainly in-plane, a mixture of d_{xy} and $d_{x^2-y^2}$, from which we expect the change of signs with the change in flip angle in our measurement geometry. A more detailed studies on the spin texture depending on the orbital characters, in both theory and experiment, as was done for the topological surface state in topological insulators [48, 49], are necessary to disentangle the nature of measured spin texture in SARPES with respect to the initial state spin.

3.5. Photon polarization dependence of the spin ARPES data

Another important aspect to consider in SARPES measurement is the polarization of incidence photons. Fig. 5 shows photon polarization dependence of the

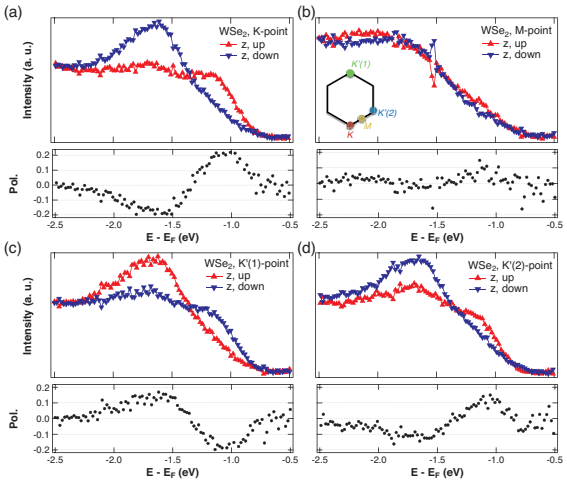

Figure 4. (Color Online) (a) - (d) Momentum dependence of the spin resolved EDCs and the spin polarization of 1ML WSe_2 at K, M, and K'(1) and K'(2) points. The inset in panel (b) shows schematic illustration of the hexagonal Brillouin zone and the definition of K, M, K'(1) and K'(2) points.

SARPES data on 1ML WSe_2 at K-point along z direction. In Fig. 5(a), one can immediately notice that spin polarization is reversed for C- polarization of incident photons, compared to the one for C+ photon polarization presented in Fig. 4(a). We observe a clear spin flip depending on the direction of rotation of the circularly polarized light. For incident photons with linear horizontal polarization, shown in Fig. 5(b), the spin polarization stays with C- photon polarization, although less pronounced particularly for the low binding energy peak.

Such spin flip with the reversal of circular light polarization, along with reduced degree of spin polarization with linear light polarization, may indicate that MX_2 could be another case for the control of photoelectron spin polarization through a change of incoming photon polarization, as shown for the topological surface state [42, 50, 51]. Such changes in spin polarization also strengthens the discussion in the previous section regarding the geometric effect due to the orbital selection rule and SARPES matrix element. As the incoming light polarization changes, the SARPES process selects only the spin polarization for outgoing photoelectrons allowed by the orbital character and associated spin texture [51]. This can gives a dramatic effect particularly for the circularly polarized light, for which the measured spin polarization can completely flip their signs.

At the same time, we also need to consider that systems with strong SOC have shown a large intensity difference as circular polarization of light gets reversed [52]. This gives a particularly interesting case for Rashba systems [53], in which such circular dichroism in ARPES signal could provide important information on the orbital angular momentum of the system. After all, the spin split VB of MX_2 is due to the combination of inversion symmetry breaking and strong SOC, and spin and orbital degrees of freedom are intricately intertwined. We cannot rule out that the observed flip of the polarization in our data is largely due to the circular dichroism, yet such dichroism could also be closely related to the initial state spin texture. Further studies on circular dichroic ARPES intensity from WSe_2 and $MoSe_2$ with varying photon energies is required to fully understand and disentangle the close relationship between spin and orbital in this system and in our SARPES data.

4. Conclusion

In conclusion, we have made SARPES measurements on a few layer samples of $MoSe_2$ and WSe_2 grown by MBE on bilayer graphene substrate. The spin polarization is found to lie mostly in out-of-plane direction with respect to the sample surface with a small amount of in-plane components. The amount of the spin polarization is much smaller than theoretically proposed due to the limited resolution and the overlap of two spin split states. With increasing thickness, the measured spin polarization disappears in 2ML but reappears in 3ML as inversion symmetry is recovered and broken again, respectively. We found the flipping of spin polarization for different valleys with geometric dependence as well as strong polarization dependence, which reveals the close coupling between orbital and spin degrees of freedom and non trivial nature of interpreting the SARPES data.

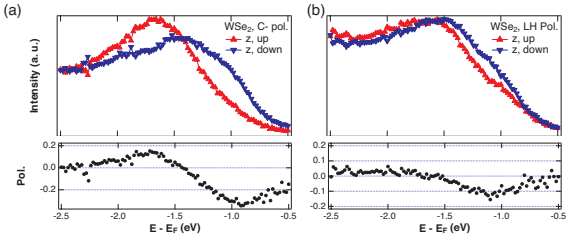

Figure 5. (Color Online) Photon polarization dependence of SARPES data from 1ML WSe_2.

References

[1] A. Geim, Science 324, 1530 (2009).
[2] R. F. Service, Science 348, 490 (2015); E. Gibney, Nature 522, 274 (2015).
[3] M. Xu, T. Liang, M. Shi, and H. Chen, Chem. Rev. (2013).
[4] M. Chhowalla, H. S. Shin, G. Eda, L.-J. Li, K. P. Loh, and H. Zhang, Nat. Chem. 5, 263 (2013).
[5] T. Ohta, A. Bostwick, T. Seyller, K. Horn, and E. Rotenberg, Science 313, 951 (2006).
[6] J. Kim, S. S. Baik, S. H. Ryu, Y. Sohn, S. Park, B.-G. Park, J. Denlinger, Y. Yi, H. J. Choi, and K. S. Kim, Science 349, 723 (2015).
[7] H. J. Conley, Bin Wang, J. I. Ziegler, R. F. Haglund, S. T. Pantelides, and K. I. Bolotin, Nano Lett. 13, 3626 (2013).
[8] A. K. Geim and I. V. Grigorieva, Nature 499, 419 (2013).
[9] E. Wang, H. Ding, A. V. Fedorov, W. Yao, Z. Li, Y.-F. Lv, K. Zhao, L.-G. Zhang, Z. Xu, J. Schneeloch, R. Zhong, S.-H. Ji, L. Wang, K. He, X. Ma, G. Gu, H. Yao, Q.-K. Xue, X. Chen, and S. Zhou, Nat. Phys. 9, 621 (2013).
[10] A. Splendiani, L. Sun, Y. Zhang, T. Li, J. Kim, C.-Y. Chim, G. Galli, and F. Wang, Nano Lett. 10, 1271 (2010).
[11] K. F. Mak, C. Lee, J. Hone, J. Shan, and T. F. Heinz, Phys. Rev. Lett. 105, 136805 (2010).
[12] M. M. Ugeda, A. J. Bradley, S.-F. Shi, F. H. da Jornada, Y. Zhang, D. Y. Qiu, W. Ruan, S.-K. Mo, Z. Hussain, Z.-X. Shen, F. Wang, S. G. Louie, and M. F. Crommie, Nat. Mater. 13, 1091 (2014).
[13] Z. Ye, T. Cao, K. O'Brien, H. Zhu, X. Yin, Y. Wang, S. G. Louie, and X. Zhang, Nature 513, 214 (2014).
[14] A. Chernikov, T. C. Berkelbach, H. M. Hill, A. Rigosi, Y. Li, O. B. Aslan, D. R. Reichman, M. S. Hybertsen, and T. F. Heinz, Phys. Rev. Lett. 113, 076802 (2014).
[15] K. F. Mak, K. He, J. Shan, and T. F. Heinz, Nat. Nanotechnol. 7, 494 (2012).
[16] H. Zeng, J. Dai, W. Yao, D. Xiao, and X. Cui, Nat. Nanotechnol. (2012).

[17] D. Xiao, G.-B. Liu, W. Feng, X. Xu, and W. Yao, Phys. Rev. Lett. 108, 196802 (2012).
[18] K. F. Mak, K. L. McGill, J. Park, and P. L. McEuen, Science 344, 1489 (2014).
[19] Z. Y. Zhu, Y. C. Cheng, and U. Schwingenschlogl, Phys. Rev. B 84, 153402 (2011).
[20] Y. Zhang, T.-R. Chang, B. Zhou, Y.-T. Cui, H. Yan, Z. Liu, F. Schmitt, J. Lee, R. Moore, Y. Chen, H. Lin, H.-T. Jeng, S.-K. Mo, Z. Hussain, A. Bansil, and Z.-X. Shen, Nat. Nanotechnol. 9, 111 (2014).
[21] Y. Zhang, M. M. Ugeda, C. Jin, S.-F. Shi, A. J. Bradley, A. Martin-Recio, H. Ryu, J. Kim, S. Tang, Y. K. Kim , B. Zhou , C. Hwang , Y. L. Chen, F. Wang, M. F. Crommie, Z. Hussain, Z.-X. Shen, and S.-K. Mo, Nano Lett. 16, 2485 (2016).
[22] L. Britnell, R. M. Ribeiro, A. Eckmann, R. Jalil, B. D. Belle, A. Mishchenko, Y. J. Kim, R. V. Gorbachev, T. Georgiou, S. V. Morozov, A. N. Grigorenko, A. K. Geim, C. Casiraghi, A. H. C. Neto, and K. S. Novoselov, Science 340, 1311 (2013).
[23] B. Radisavljevic, A. Radenovic, J. Brivio, V. Giacometti, and A. Kis, Nat. Nanotechnol. 6, 147 (2011).
[24] O. Lopez-Sanchez, D. Lembke, M. Kayci, A. Radenovic, and A. Kis, Nat. Nanotechnol. (2013).
[25] A. Damascelli, Z. Hussain, and Z. X. Shen, Rev. Mod. Phys. 75, 473 (2003).
[26] T. Eknapakul, P. D. C. King, M. Asakawa, P. Buaphet, R. H. He, S.-K. Mo, H. Takagi, K. M. Shen, F. Baumberger, T. Sasagawa, S. Jungthawan, and W. Meevasana, Nano Lett. 14, 1312 (2014).
[27] N. Alidoust, G. Bian, S.-Y. Xu, R. Sankar, M. Neupane, C. Liu, I. Belopolski, D.-X. Qu, J. D. Denlinger, F.-C. Chou, and M. Z. Hasan, Nat. Commun. 5, 4673 (2014).
[28] D. W. Latzke, W. Zhang, A. Suslu, T.-R. Chang, H. Lin, H.-T. Jeng, S. Tongay, J. Wu, A. Bansil, and A. Lanzara, Phys. Rev. B 91, 235202 (2015).
[29] W. Jin, P.-C. Yeh, N. Zaki, D. Zhang, J. T. Sadowski, A. Al-Mahboob, A. M. van der Zande, D. A. Chenet, J. I. Dadap, I. P. Herman, P. Sutter, J. Hone, and R. M. Osgood, Phys. Rev. Lett. 111, 106801 (2013).
[30] J. A. Miwa, S. Ulstrup, S. G. Sørensen, M. Dendzik, A. G. Čabo, M. Bianchi, J. V. Lauritsen, and P. Hofmann, Phys. Rev. Lett. 114, 046802 (2015).
[31] J. Osterwalder, J. Phys.: Condens. Matter 24, 171001 (2012).
[32] J. H. Dil, J. Phys.: Condens. Matter 21, 403001 (2009).
[33] U. Heinzmann and J. H. Dil, J. Phys.: Condens. Matter 24, 173001 (2012).
[34] D. Hsieh, Y. Xia, L. Wray, D. Qian, A. Pal, J. H. Dil, J. Osterwalder, F. Meier, G. Bihlmayer, C. L. Kane, Y. S. Hor, R. J. Cava, and M. Z. Hasan, Science 323, 919 (2009).
[35] C. Jozwiak, Y. Chen, A. Fedorov, J. Analytis, C. Rotundu, A. Schmid, J. Denlinger, Y. D. Chuang, D. H. Lee, I. Fisher, R. Birgeneau, Z. X. Shen, Z. Hussain, and A. Lanzara, Phys. Rev. B 84, 165113 (2011).
[36] J. Sánchez-Barriga, A. Varykhalov, J. Braun, S. Y. Xu, N. Alidoust, O. Kornilov, J. Minár, K. Hummer, G. Springholz, G. Bauer, R. Schumann, L. V. Yashina, H. Ebert, M. Z. Hasan, and O. Rader, Phys. Rev. X 4, 011046 (2014).
[37] R. Suzuki, M. Sakano, Y. J. Zhang, R. Akashi, D. Morikawa, A. Harasawa, K. Yaji, K. Kuroda, K. Miyamoto, T. Okuda, K. Ishizaka, R. Arita, and Y. Iwasa, Nat. Nanotechnol. 9, 611 (2014).
[38] H. Coy Diaz, F. Bertran, C. Chen, J. Avila, J. Rault, P. Fèvre, M. C. Asensio, and M. Batzill, Phys. Status Solidi RRL 9, 701 (2015).
[39] J. M. Riley, F. Mazzola, M. Dendzik, M. Michiardi, T. Takayama, L. Bawden, C. Granerød, M. Leandersson, T. Balasubramanian, M. Hoesch, T. K. Kim, H. Takagi, W. Meevasana, P. Hofmann, M. S. Bahramy, J. W. Wells, and P. D. C. King, Nat. Phys. 10, 835 (2014).
[40] M. Hoesch, T. Greber, V. N. Petrov, M. Muntwiler, M. Hengsberger, W. Auwrter, and J. Osterwalder, J. Electron. Spectrosc. Relat. Phenom. 124, 263 (2002).
[41] F. Meier, V. Petrov, H. Mirhosseini, L. Patthey, J. Henk, J. Osterwalder, and J. Hugo Dil, J. Phys.: Condens. Matter 23, 072207 (2011).
[42] Z. H. Zhu, C. N. Veenstra, S. Zhdanovich, M. P. Schneider, T. Okuda, K. Miyamoto, S. Y. Zhu, H. Namatame, M. Taniguchi, M. W. Haverkort, I. S. Elfimov, and A. Damascelli, Phys. Rev. Lett. 112, 076802 (2014).
[43] M.-Y. Li, Y. Shi, C.-C. Cheng, L.-S. Lu, Y.-C. Lin, H.-L. Tang, M.-L. Tsai, C.-W. Chu, K.-H. Wei, J.-H. He, W.-H. Chang, K. Suenaga, and L.-J. Li, Science 349, 524 (2015).
[44] S. Helveg, J. Lauritsen, E. Lægsgaard, I. Stensgaard, J. Nørskov, B. Clausen, H. Topsøe, and F. Besenbacher, Phys. Rev. Lett. 84, 951 (2000).
[45] H. Liu, L. Jiao, F. Yang, Y. Cai, X. Wu, W. Ho, C. Gao, J. Jia, N. Wang, H. Fan, W. Yao, and M. Xie, Phys. Rev. Lett. 113, 066105 (2014).
[46] S. Barja, S. Wickenburg, Z.-F. Liu, Y. Zhang, H. Ryu, M. M. Ugeda, Z. Hussain, Z.-X. Shen, S.-K. Mo, E. Wong, M. B. Salmeron, F. Wang, M. F. Crommie, D. F. Ogletree, J. B. Neaton, and A. Weber-Bargioni, Nat. Phys., in press (2016). (doi:10.1038/nphys3730)
[47] G. Landolt, Spin- and Angle-Resolved Photoelectron Spectroscopy on Topological Insulators and Bulk Rashba Systems, Ph. D. Dissertation, Universität Zürich (2014).
[48] H. Zhang, C.-X. Liu, and S.-C. Zhang, Phys. Rev. Lett. 111, 066801 (2013).
[49] Y. Cao, J. A. Waugh, X.-W. Zhang, J.-W. Luo, Q. Wang, T. J. Reber, S.-K. Mo, Z. Xu, A. Yang, J. Schneeloch, G. D. Gu, M. Brahlek, N. Bansal, S. Oh, A. Zunger, and D. S. Dessau, Nat. Phys. 9, 499 (2013).
[50] C. Jozwiak, C.-H. Park, K. Gotlieb, C. Hwang, D.-H. Lee, S. G. Louie, J. D. Denlinger, C. R. Rotundu, R. J. Birgeneau, Z. Hussain, and A. Lanzara, Nat. Phys. 9, 293 (2013).
[51] C.-H. Park and S. G. Louie, Phys. Rev. Lett. 109, 097601 (2012).
[52] S. R. Park, J. Han, C. Kim, Y. Y. Koh, C. Kim, H. Lee, H. J. Choi, J. H. Han, K. D. Lee, N. J. Hur, M. Arita, K. Shimada, H. Namatame, and M. Taniguchi, Phys. Rev. Lett. 108, 046805 (2012).
[53] B. Kim, P. Kim, W. Jung, Y. Kim, Y. Koh, W. Kyung, J. Park, M. Matsunami, S.-I. Kimura, J. S. Kim, J. H. Han, and C. Kim, Phys. Rev. B 88, 205408 (2013).

Acknowledgments

The work at the ALS is supported by the US DOE, Office of Basic Energy Science, under contract No. DE-AC02-05CH11231. The work at the Stanford Institute for Materials and Energy Sciences and Stanford University is supported by the US DOE, Office of Basic Energy Sciences, under contract No. DE-AC02-76SF00515. The work at Pusan National University is supported by the National Research Foundation of Korea (NRF) funded by the Ministry of Science, ICT, and Future Planning (No. 2015R1C1A1A01053065). The work at the EPFL is supported by Swiss National Science Foundation (PP00P2_144742/1).